Analytical Methods

RSC Publishing

PAPER

View Article Online
View Journal | View Issue

Cite this: *Anal. Methods*, 2013, **5**, 4666

Alkali metal ions transfer across the water/1,2-dichloroethane interface facilitated by a series of crown ethers†

Girum Girma,[a] Li-Juan Yu,[a] Li Huang,[a] Shan Jin,*[b] De-Yin Wu[a] and Dongping Zhan*[a]

Received 17th April 2013
Accepted 23rd June 2013

DOI: 10.1039/c3ay40643a

www.rsc.org/methods

The facilitated transfer of alkali metal ions (Li^+ and Na^+) across the water/1,2-dichloroethane (W/1,2-DCE) interface was studied by using a series of crown ethers as ionophores: 4′-ethynylbenzo-15-crown-5-ether (**L1**), 3′,6′-diethynylbenzo-15-crown-5-ether (**L2**) and 4′,5′-diethynylbenzo-15-crown-5-ether (**L3**). Cyclic voltammetry was employed to study the electrochemical behaviour of the facilitated ion transfer across the W/1,2-DCE interface supported at the tip of a micropipette. The diffusion coefficients of the ionophores in the 1,2-DCE phase were determined, while the metal–ligand complexes formed by these ions with all the ionophores were obtained to be in a 1 : 1 stoichiometric ratio. The association constants, log β°, for complexes Li**L1**$^+$, Li**L2**$^+$, Li**L3**$^+$, Na**L1**$^+$, Na**L2**$^+$ and Na**L3**$^+$ were calculated to be 3.3, 4.2, 4.0, 2.1, 3.5 and 2.2, respectively. The theoretical calculations have shown that the conjugated constituent groups on the benzene ring have an essential effect on the spatial structures of the crown ether rings, which determine the supramolecular interaction between the ions and ionophores.

Introduction

When two immiscible liquids contact with each other, they form an interface of mixed boundary in between them, which is known as the liquid–liquid (L/L) interface, which separates the two bulk liquid phases. At the L/L interface, various physico-chemical processes take place, such as molecular partition based on the difference of solvation energy in each phase, and the change of interfacial structure in response to environmental factors (temperature, pressure and components of the adjacent bulk phases). If one or both bulk liquid phases contain ions, the partition coefficient of the ion is relevant to the interfacial potential difference.[1] On the other hand, the interfacial potential difference plays an important role in driving the ion transfer across the liquid–liquid interface, which can generate Faraday current and be observed electrochemically. In general, there are two types of ion transfer across the L/L interface, namely simple ion transfer (IT), which involves the change of solvation energy, and facilitated ion transfer (FIT), which encompasses an ion transfer coupled with an interfacial complexation reaction between the ion and its ionophore or ligand.[2] If there is a hydrophobic ionophore in the organic phase, the Gibbs energy of the ion transfer will be lowered due to the interfacial complexation reaction. Consequently, the ion transfer across the L/L interface will be "facilitated".[3]

IT and FIT across the L/L interface are heterogeneous charge transfer processes which have crucial roles in electrochemistry, analytical chemistry and membrane sciences.[4,5] They have been widely studied because of supramolecular chemistry as well as their relevance to many important chemical and biological systems.[6] The ion transfer across the L/L interface, including inorganic and organic species and biological substances, can be investigated by electrochemical methods. The key benefit of electrochemistry at the L/L interface is that it allows for the analytical detection of ions even if they do not undergo any redox reaction. Furthermore, the miniaturization of the L/L interfacial area to the micro- and nano-meter size has given crucial advantages in reducing the interfacial capacity of electrical double layers and the IR drop in the resistive organic phase.[3,7] Thus, the L/L interface has become an important branch of modern electroanalytical chemistry.

After Koryta *et al.* described the electrochemical polarizability of the L/L interface and the discovery by Pedersen of crown ethers as ion carriers, extensive attention has been paid to FIT by ionic ligands or ionophores.[8–12] Among the ionophores developed so far for molecular recognition purposes are mainly crown ethers and their derivatives, which have been proven to have good ion binding capabilities. Since the crown ethers are hard bases, they can effectively bind with hard acids of group I and II metal ions to form stable complexes.[13] The interior of the

[a]*State Key Laboratory for Physical Chemistry of Solid Surfaces, College of Chemistry and Chemical Engineering, Xiamen University, Xiamen 361005, China. E-mail: dpzhan@xmu.edu.cn; Fax: +86-592-2181906; Tel: +86-592-2185797*

[b]*Key Laboratory of Pesticide and Chemical Biology, Ministry of Education, College of Chemistry, Central China Normal University, Wuhan 430079, P.R. China. E-mail: jinshan@mail.ccnu.edu.cn; Fax: +86-27-67867141; Tel: +86-13035100069*

† Electronic supplementary information (ESI) available: Theoretical calculation details for the supramolecular interactions between the ions and ionophores. See DOI: 10.1039/c3ay40643a

crown ethers is highly hydrophilic and electron rich due to the presence of lone-pairs of electrons on the ring oxygen atoms, which share the charge of the ion to form a stable complex. This phenomenon is called the supramolecular effect and is distinct from the traditional chemical bond. Due to the interfacial supramolecular effect, ion transfer from the aqueous phase to a highly hydrophobic organic phase is facilitated. It should be noted that the size compatibility and the delocalized interaction between the ionophore and the ion play important roles in the selectivity and sensitivity of the ionophore to the ion of interest. In this work, a series of benzo-15-crown-5 derivatives, including 4′-ethynylbenzo-15-crown-5-ether (**L1**), 3′,6′-diethynylbenzo-15-crown-5-ether (**L2**) and 4′,5′-diethynylbenzo-15-crown-5-ether (**L3**), are tested to facilitate the transfer of alkali metal ions across a micropipette supported water/1,2-dichloroethane (W/1,2-DCE) interface. The molecular structures of these crown ethers are depicted in Fig. 1.

Experimental section

Fabrication of micropipettes

The borosilicate glass capillaries with internal and external diameters of 0.58 mm and 1 mm were used for the fabrication of micropipettes with a micrometer-sized orifice, which were pulled using the P-2000 laser puller (Sutter Instrument Co., USA). By choosing appropriate programs and adjusting the parameters (heat, filament, velocity, and delay) followed by holding the glass capillary properly on the pipette clamp, two micropipettes with identical orifices could be obtained at the same time. The need for adjusting the appropriate pulling parameters is to ensure the micropipettes have a short shank and flat vent.[2,14] An optical microscope (BX-51, Olympus, Japan) and a digital microscope (KEYENCE, VHX-600, USA) were used to verify the quality of pulled micropipettes and to measure the radius of the tip orifice.

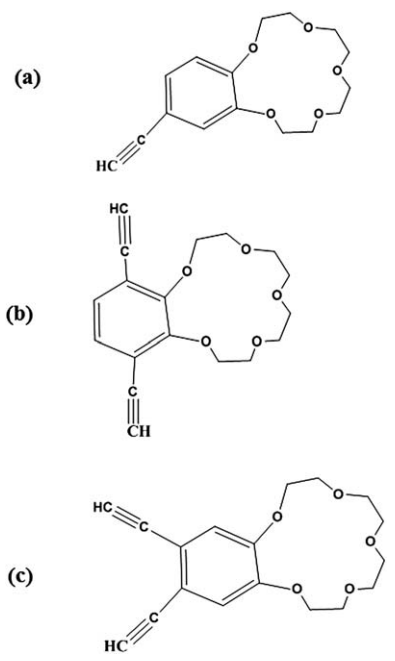

Fig. 1 Molecular structures of ionophores (a) 4′-ethynylbenzo-15-crown-5-ether (**L1**) (b) 3′,6′-diethynylbenzo-15-crown-5-ether (**L2**) and (c) 4′,5′-diethynylbenzo-15-crown-5-ether (**L3**).

Chemicals

The ionophores, 4′-ethynylbenzo-15-crown-5-ether, 3′,6′-diethynyl-benzo-15-crown-5-ether and 4′,5′-diethynylbenzo-15-crown-5-ether were synthesized and purified in our lab. Lithium chloride (LiCl), sodium chloride (NaCl), 1,2-dichloroethane (1,2-DCE) and tetrabutylammonium tetraphenylborate (TBATPB) were provided by Sinopharm Co., China. The purity of TBATPB was 98% and was used as the supporting electrolyte in the organic phase. All the chemicals used were of analytical grade or better. The aqueous solutions were prepared by using deionized water (18.2 MΩ cm^{-1}, Milli-Q, Millipore Corp.).

Electrochemical measurements

All electrochemical experiments were performed with a CHI 760D electrochemical work station (CH Instruments Inc., USA). The aqueous solution was injected into the micropipette and immersed in the 1,2-DCE solution to form the micrometer-sized L/L interface. A two-electrode system was adapted as described by Beattie and co-workers.[15] A silver wire (diameter: 125 μm) coated with AgCl was inserted into the micropipette and acted as the reference electrode in the aqueous phase. Another silver wire coated with AgTPB was used as the reference electrode in the outer organic solution. The experiments were conducted at room temperature (23 ± 2 °C). The electrochemical cells used in this work can be represented as:

$$\text{Ag/AgTPB/}x\text{ mM }\mathbf{L}\text{ + 5 mM TBATPB (1,2-DCE)//}y\text{ mM MCl (W)/AgCl/Ag}$$

Where **L** stands for the ionophores, MCl represents NaCl or LiCl, x and y are the concentrations of ionophores and MCl respectively. To determine the thermodynamic parameters, TMA^+ (tetramethylammonium) was used as the inner reference, and $\Delta_o^w\varphi_{TMA^+} = 160$ mV was used as the standard Galvani potential difference for TMA^+ transfer across the water/1,2-DCE interface based on the TATB assumption.[16]

Results and discussion

The electrochemical behaviour of lithium and sodium ion transfer across the micropipette supported W/1,2-DCE interface facilitated by **L1** is shown in Fig. 2. The concentration of lithium and sodium ions is 200 mM while the concentrations of **L1** are 0.75, 1.0, 1.5 and 2.0 mM, respectively. The concentration of the alkali ions in the aqueous phase is much higher than that of **L1** in the 1,2-DCE phase. In this case, the IR drop in the aqueous phase can be neglected and the potential distributes mainly in the 1,2-DCE phase. Meanwhile, the rate-determining step is the diffusion of the ionophore in the organic phase. The micropipette supported W/1,2-DCE interface behaves just like a disk

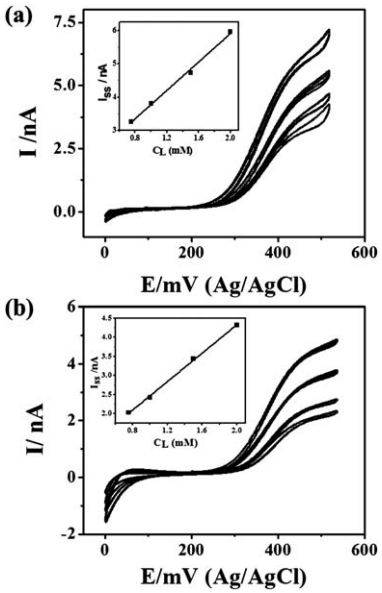

Fig. 2 The steady-state voltammograms of the facilitated transfer of (a) 200 mM Li^+, (b) 200 mM Na^+ ions by 0.75, 1, 1.5 and 2 mM of **L1** across the micropipette supported water/1,2-DCE interface. The average radius of the micropipette tip used is 4.9 μm and the scan rate is 100 mV s^{-1}. The insets in (a) and (b) show the linear relation between the steady-state current and the concentration of ionophore **L1**.

ultra-microelectrode. As pointed out by Shao *et al.*, there exists an asymmetric diffusion layer for species transferring inside and outside the micropipette orifice, which results in special voltammetric behaviours.[17] The transfer mechanism can be figured out from the shape of the voltammograms. As shown in Fig. 2, both the anodic and cathodic current responses present well-defined characteristics of a diffusion controlled steady-state. It can be concluded that the mechanism of lithium and sodium ion transfer by **L1** is a TIC (transfer by interfacial complex)/TID (transfer by interfacial dissociation) process.[18]

The semi-logarithmic relationship between the applied potential at the interface, E and $\log((i_{ss} - i)/i)$ is linear with a slope of 60.4 mV per decade for the lithium ion and 63.3 mV per decade for the sodium ion, which indicates that the FIT processes are pretty reversible with a charge transfer number of 1. The limiting steady-state current is in proportion to the concentration of **L1** in the 1,2-DCE phase (the insets in Fig. 2a and b), which abide by the following equation:

$$i_{ss} = 3.35\pi nFDCa \quad (1)$$

where i_{ss} is the limiting steady-state current, n the transferred charge number, F the Faraday constant, D the diffusion coefficient of the ionophore in 1,2-DCE, C the concentration of the ionophore, and a the radius of the orifice of the micropipette. The diffusion coefficient of **L1** can be obtained through eqn (1). The FIT of lithium and sodium ions by ionophore **L2** and **L3** have similar behaviours to that of ionophore **L1**. The diffusion coefficients obtained are listed in Table 1. Even if the D values of each ionophore in the case of lithium and sodium ions are a little bit different, they are reasonable within the error range.

Table 1 The slopes for the E *versus* $\log((i_{ss} - i)/i)$ plots for the three ionophores facilitating the transfer of Li^+ and Na^+ ions and the diffusion coefficients in the 1,2-DCE phase

	Slope		D (10^{-6} cm^2 s^{-1})	
Ligand	Li^+	Na^+	Li^+	Na^+
L1	60.4	63.3	3.9	3.6
L2	59.6	65.2	1.3	1.5
L3	63.5	62.0	1.6	2.0

One of the advantages of voltammetry of FIT at the L/L interface is that it is relatively easy to obtain the association constants and other thermodynamic data without traditional experimental procedures including reflux, separation and elemental analysis. For a reversible FIT process controlled by the diffusion of an ionophore in the organic phase, the following equation can be deduced for a 1 : 1 complexation:[19]

$$\Delta_o^w\varphi_{1/2,M^{z+}} = \Delta_o^w\varphi_{M^{z+}}^{o'} + \frac{RT}{zF}\ln\frac{D_L}{D_{ML^+}} - \frac{RT}{zF}\ln\beta^\circ C_{M^{z+}}^W \quad (2)$$

where $\Delta_o^w\varphi_{1/2,M^{z+}}$ is the half-wave potential of the FIT at the L/L interface, $\Delta_o^w\varphi_{M^{z+}}^{o'}$ is the formal potential of metal ion transfer at the L/L interface, D_L and D_{ML^+} are the diffusion coefficients of the ionophore and the ion–ionophore complex, ln β° is the association constant of ML, $C_{M^{z+}}^W$ is the concentration of the ion in the aqueous phase and the other symbols have their normal definitions. Eqn (2) can be used to obtain the association constant of the interfacial reaction between the ion in aqueous solution and the ionophore in organic solution.

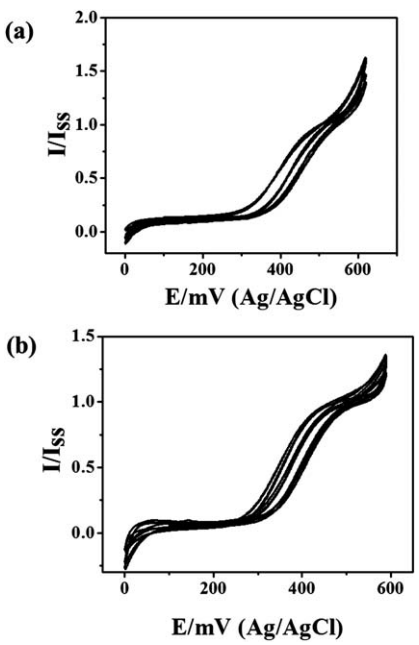

Fig. 3 The overlaid steady state cyclic voltammograms obtained for the transfer of (a) Li^+ and (b) Na^+ ions across micropipette supported water/1,2-DCE interfaces facilitated by 2 mM of **L1**. The concentrations of the ions (Li^+ and Na^+) are 100, 200, 300 and 400 mM for both ions. The voltage scan rate is 100 mV s^{-1} for all cases.

The voltammograms shown in Fig. 3 show the FIT potential shift with the change in concentration of lithium and sodium ions in the aqueous phase. The linear relationships between the half-wave potential of FIT and the logarithm of the ion concentration in the aqueous phase are shown in Fig. 4. Considering the potential of the Ag/AgCl reference electrode changes with the concentration of chloride ion in the aqueous phase, this linear relationship should have an expected slope of 116 mV per decade at ambient temperature. All the obtained data are listed in Table 2. From the experimental slopes it can be concluded that the stoichiometric ratios of the ionophores to lithium and sodium ions are 1 : 1. With potential correction by the TATB hypothesis, the association constants between the ions and ionophores are listed in Table 2.

Density functional calculations were carried out with Becke's three-parameter hybrid exchange functional and the Lee–Yang–Parr correlation functional approach B3LYP.[20–23] The basis sets for C, O, H, Li and Na atoms of the investigated molecules were 6-311+G(d, p), which included the polarization function in all the atoms and diffuse function in C, O, Li and Na atoms.[24,25] The polarizable continuum model (PCM) was used in our system and dichloroethane with a dielectric constant, ε, of 10.125 was chosen as solvent.[20] All the quantum chemical calculations, including geometry optimizations, bond distances and charge distributions were carried out by using the Gaussian 09 package.[26] All the details are shown in the ESI.†

Considering the sizes of the cations, Li^+ is smaller than Na^+. Consequently, the Li^+ ion has a greater polarizing effect on the nearby atoms than the Na^+ ion. Therefore, the Li^+ ion is supposed to have a more strongly polarizing effect on the C–O bonds of the crown rings than the Na^+ ion. This polarization gives the variation of charge distribution on the complexes. Thus, the complexes of the Li^+ ion with all ionophores are found to be more stable than those of the Na^+ ion, which results in the higher association constants of the Li**L** complexes. The comparison among the ionophores (benzo-15-crown-5-ethers) with each other has shown that the charge distribution on the oxygen atoms of the crown ring of **L3** changes more than that of **L1** and **L2**. Experimentally, the difference between the log β° values is the largest, which indicates a higher selectivity of **L3** to Li^+ ion than to Na^+ ion.[27] All the results of theoretical calculations are verified by the experimental results.

Furthermore, in view of the size effect, B15C5 derivatives should have a greater affinity to the Na^+ ion. However, the experimental results show that the complexes of these ionophores are stronger with the Li^+ ion than with the Na^+ ion. Theoretical calculations also show that both the distances between the ring oxygens and the effective charges of each ring oxygen atom are changed when the ionophores complex with the alkali ions. It can be concluded that the self-organization effect of the ion–ionophore complex plays a significant role in the supramolecular interaction.

Table 2 The parameters determined from the $E_{1/2,M^+}$ *versus* log C_{M^+} plots for the transfer of Li^+ and Na^+ ions facilitated by the series of ionophores (**L1**, **L2** and **L3**)

Ligand	Ion	Slope	Intercept	Log β°	$M : L$
L1	Li^+	−116.6	462.7	3.3	1 : 1
	Na^+	−112.0	415.3	2.1	1 : 1
L2	Li^+	−111.6	447.2	4.0	1 : 1
	Na^+	−117.6	379.7	3.5	1 : 1
L3	Li^+	−113.5	447.2	4.2	1 : 1
	Na^+	−112.0	374.0	2.2	1 : 1

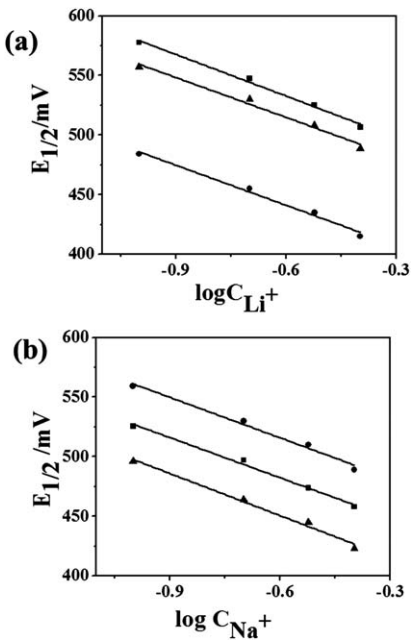

Fig. 4 The half-wave potential $E_{1/2}$ *versus* log C_{M^+} plot for the facilitated transfer of (a) Li^+ and (b) Na^+ ions across the micropipette supported water/1,2-DCE interface assisted by the ionophore **L1** (■), **L2** (▲) and **L3** (●).

Conclusions

Electrochemistry at the liquid–liquid interface has proved an effective analytical method for the thermodynamic investigation of the supramolecular interaction between ion and ionophore. Theoretical calculation results show that self-organization plays a greater role than the simple size effect because the ring structure does change in the complex reaction.

Acknowledgements

The financial support of the National Basic Research Program of China (2011CB933700, 2012CB932900), the National Science Foundation of China (NSFC21061120456, 21021002, 20973142), and the National Project 985 of High Education are appreciated. Especially, G. Girma thanks the financial support of Chinese Government Scholarship for his International Master program.

References

1 F. Scholz, *Annu. Rep. Prog. Chem., Sect. C*, 2006, **102**, 43.
2 S. Liu, Q. Li and Y. Shao, *Chem. Soc. Rev.*, 2011, **40**, 2236.
3 Y. Yuan, Z. Gao, J. Guo and Y. Shao, *J. Electroanal. Chem.*, 2002, **526**, 85.

4 E. Torralba, A. Molina, C. Serna and J. A. Ortuño, *Int. J. Electrochem. Sci.*, 2012, **7**, 6771.
5 Z. Samec, *Pure Appl. Chem.*, 2004, **76**, 2147.
6 Y. Wang, J. Velmurugan, M. V. Mirkin, P. J. Rodgers, J. Kim and S. Amemiya, *Anal. Chem.*, 2009, **82**, 77.
7 J. Strutwolf, M. D. Scanlon and D. W. M. Arrigan, *Analyst*, 2009, **134**, 148.
8 J. Koryta, *Electrochim. Acta*, 1979, **24**, 293.
9 C. Schalley, *Analytical methods in supramolecular chemistry*, Wiley-VCH, 2nd edn, 2012.
10 B. Su and Y. Shao, *Chin. Sci. Bull.*, 2002, **47**, 1325.
11 D. Zhan, Y. Xiao, Y. Yuan, Y. He, B. Wu and Y. Shao, *J. Electroanal. Chem.*, 2003, **553**, 43.
12 D. Zhan, Y. Yuan, Y. Xiao, B. Wu and Y. Shao, *Electrochim. Acta*, 2002, **47**, 4477.
13 S. Fery-Forgues and F. Al-Ali, *J. Photochem. Photobiol., C*, 2004, **5**, 139.
14 Y. Qiao, B. Zhang, X. Zhu, T. Ji, B. Li, Q. Li, E. Chen and Y. Shao, *Electroanalysis*, 2013, **25**, 1.
15 P. D. Beattie, A. Delay and H. H. Girault, *J. Electroanal. Chem.*, 1995, **380**, 167.
16 S. Wilke and T. Zerihun, *J. Electroanal. Chem.*, 2001, **515**, 52.
17 Y. Shao and M. V. Mirkin, *J. Am. Chem. Soc.*, 1997, **119**, 8103.
18 Y. Shao, M. D. Osborne and H. H. Girault, *J. Electroanal. Chem.*, 1991, **318**, 101.
19 H. Matsuda, Y. Yamada, K. Kanamori, Y. Kudo and Y. Takeda, *Bull. Chem. Soc. Jpn.*, 1991, **64**, 1497.
20 J. Tomasi, B. Mennucci and R. Cammi, *Chem. Rev.*, 2005, **105**, 2999.
21 A. D. Becke, *J. Chem. Phys.*, 1993, **98**, 5648.
22 A. D. Becke, *J. Chem. Phys.*, 1996, **104**, 1040.
23 C. Lee, W. Yang and R. G. Parr, *Phys. Rev. B*, 1988, **37**, 785–789.
24 P. Gao and M. J. Weaver, *J. Phys. Chem.*, 1985, **89**, 5040.
25 M. Muniz-Miranda, B. Pergolese and A. Bigotto, *J. Phys. Chem. C*, 2008, **112**, 6988.
26 M. Frisch, G. Trucks, H. Schlegel, G. Scuseria, M. Robb, J. Cheeseman, G. Scalmani, V. Barone, B. Mennucci and G. Petersson, *Gaussian 09 Revision A. 02*, Gaussian Inc., Wallingford CT, 2009.
27 J. Wang, *Anakytical Electrochemistry*, Wiley-VCH, 2nd edn, 2001.

